

Strain engineering of self-organized InAs quantum dots

F. Guffarth,¹ R. Heitz,¹ A. Schliwa,¹ O. Stier,¹ N. N. Ledentsov,^{1,*} A. R. Kovsh,² V. M. Ustinov,² and D. Bimberg¹

¹*Institut für Festkörperphysik, Technische Universität Berlin, Hardenbergstraße 36, D-10623 Berlin, Germany*

²*A. F. Ioffe Physicotechnical Institute, Russian Academy of Sciences, St. Petersburg, Russia*

(Received 15 February 2001; published 1 August 2001)

The effects of a thin gallium-rich $\text{In}_x\text{Ga}_{1-x}\text{As}$ cap layer on the electronic properties of self-organized InAs quantum dots (QD's) are investigated both experimentally and theoretically. Increasing the indium concentration of the cap layer allows tuning the ground state transition to lower energies maintaining strong quantization of the electronic states. Strain-driven partial decomposition of the $\text{In}_x\text{Ga}_{1-x}\text{As}$ cap layer increases the effective QD size during growth and the altered barrier composition leads to a partial strain relaxation within the capped InAs QD's. Strain engineering the structural properties of the QD's as well as the actual confining potential offers a pathway to control the electronic properties, e.g., to shift the emission wavelength of lasers based on self-organized InAs QD's to the infrared.

DOI: 10.1103/PhysRevB.64.085305

PACS number(s): 78.67.Hc, 78.55.Cr, 73.21.La, 73.61.Ey

I. INTRODUCTION

In recent years self-organized quantum dots (QD's) have evolved as a model system for the study of the fundamental physics of zero-dimensional systems.¹ Devices like QD lasers and detectors are based on such self-organized QD's.²⁻⁵ Controlled tuning of the electronic properties of such QD's is, however, still a challenge due to the intricate dependencies of the QD density, size, and shape in the self-organized growth. One way to modify the electronic properties of self-organized QD's is annealing-induced interdiffusion.^{6,7} The resulting QD potential becomes shallower and softer, shifting the ground state transition to *higher* energy and reducing the lateral confinement, i.e., the quantization, respectively. Control of island formation and evolution during growth is obtained, e.g., by exploiting strain-modified surface kinetics in multilayered samples,^{8,9} i.e., vertical self-organization of island stacks. For example, small QD's in a "seed" layer can be used as stressors to control independently the island size and density in subsequent layers.¹⁰ The formation of increasingly large islands with increasing deposition amount leads to a pronounced *low-energy* shift of the ground state transition energy, allowing one to achieve, e.g., 1.3 μm emission at room temperature with InAs/GaAs QD's.¹¹ However, the increasing QD size correlates to a decreasing quantization¹²⁻¹⁴ and the increasing strain hampers high-quality stacking.

The overgrowth of self-organized InAs QD's with an $\text{In}_x\text{Ga}_{1-x}\text{As}$ layer has recently been demonstrated as effective means to tune the ground state transition to the 1.3 μm spectral region.¹⁵ The structural and electronic properties of the resulting QD structures are, however, poorly understood. Overgrowth by a gallium-rich $\text{In}_x\text{Ga}_{1-x}\text{As}$ layer alters the electronic properties of the InAs/GaAs quantum structure in three interrelated ways.

(1) First, strain-driven surface kinetics leads to a partial decomposition of the $\text{In}_x\text{Ga}_{1-x}\text{As}$ layer during growth¹⁶ due to preferential incorporation of indium at already existing InAs islands, thus increasing the effective QD size.

(2) Second, the $\text{In}_x\text{Ga}_{1-x}\text{As}$ cap layer allows for more

efficient strain relaxation,¹⁷⁻¹⁹ altering the electronic potential of the capped QD's.

(3) Finally, the low-energy quantum well (QW) formed by the original InAs wetting layer (WL) and the partly decomposed $\text{In}_x\text{Ga}_{1-x}\text{As}$ layer lowers the lateral confinement, reducing the number of localized states and enhancing lateral coupling between the QD's at finite temperatures.

As shown recently,²⁰ the degree of decomposition of the $\text{In}_x\text{Ga}_{1-x}\text{As}$ cap layer depends on the indium composition x , the size of the initial InAs islands, and the growth conditions. The strain distribution in the overgrown structure depends on the actual indium content and the thickness of the $\text{In}_x\text{Ga}_{1-x}\text{As}$ cap layer. Thus, this type of growth approach provides the potential to strain engineer the structural and electronic properties of self-organized QD's. Additionally, the $\text{In}_x\text{Ga}_{1-x}\text{As}$ layer reduces the inhomogeneous surface stress and therefore the strain interaction with subsequent QD layers, enhancing the ability to grow a multitude of identical uncorrelated QD layers.²⁰ A high volume density of QD's is needed, e.g., for large quantum efficiency laser devices.¹⁵ The utilization of the full potential of this innovative growth approach requires a quantitative understanding of the interrelated effects on the electronic properties.

Here, we report on a photoluminescence (PL) and PL excitation (PLE) study of InAs QD's capped by an $\text{In}_x\text{Ga}_{1-x}\text{As}$ layer of varying nominal indium concentration. In order to obtain a detailed understanding of the resulting complex quantum structure the results are compared to transmission electron microscopy (TEM) data,²⁰ eight-band $\mathbf{k}\cdot\mathbf{p}$ calculations of the zero-dimensional QD states, and effective mass calculations for the two-dimensional QW states. Quantitative insight into the contributions of partial decomposition and strain relaxation to the observed low-energy shift with increasing indium concentration of the $\text{In}_x\text{Ga}_{1-x}\text{As}$ layer is obtained.

II. EXPERIMENT

The investigated samples were grown by solid-source molecular beam epitaxy on GaAs(001) substrate as described

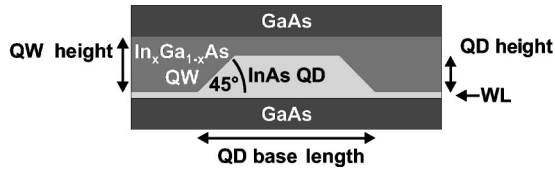


FIG. 1. Schematic of the QD sample structure.

in detail in Ref. 20. First, an AlAs/GaAs superlattice followed by 100 nm GaAs were grown at 600 °C. Subsequently, the temperature was lowered to 485 °C for the deposition of ~ 2.1 monolayers (ML) of InAs forming the initial InAs islands. The islands were capped by a 4 nm thick $\text{In}_x\text{Ga}_{1-x}\text{As}$ layer with an indium composition x of up to 25% followed by 10 nm GaAs. (For $x=0$, 2.3 ML InAs were deposited for the initial InAs islands which affects mainly the QD density.) Finally, the temperature was raised to 600 °C for the growth of 10 nm GaAs, an AlAs/GaAs superlattice, and a 5 nm GaAs protection layer. The lateral density of the QD's determined from plan-view TEM images was in the range of $400 \mu\text{m}^{-2}$ to $900 \mu\text{m}^{-2}$ for the various samples. A sketch of the QD's in the InAs/ $\text{In}_x\text{Ga}_{1-x}\text{As}$ structures is shown in Fig. 1. The InAs QD's are embedded in a QW formed by the original InAs WL and the $\text{In}_x\text{Ga}_{1-x}\text{As}$ cap layer. For the investigated samples TEM results²⁰ suggest a flat truncated shape of the overgrown InAs QD's with a base length between ~ 12 nm and ~ 14 nm and an estimated height around 3 nm. The average size of the InAs QD's increases monotonically on increasing the indium concentration of the cap layer from 0 to 20% (see the inset of Fig. 6 in Ref. 20). For the investigated samples the growth parameters were chosen so as to minimize the decomposition of the $\text{In}_x\text{Ga}_{1-x}\text{As}$ layer, in order to quantify the concomitant effect of strain relaxation in such structures.

The PL and PLE experiments were performed in a continuous-flow He cryostat at 7 K. A tungsten lamp dispersed by an 0.27 m double-grating monochromator served as a low-density, tunable light source. The emission was spectrally dispersed by an 0.3 m double-grating monochromator and detected with a cooled Ge diode using lock-in techniques.

III. EXPERIMENTAL RESULTS

Figure 2 compares low-temperature PL spectra (dashed lines) of the series of samples taken at low excitation density (~ 5 mW/cm²). The most prominent effect is a pronounced redshift of the ground state transition on increasing the indium concentration from $x=0$ to $x=20\%$ despite the only small increase of the average size of the QD's.²⁰ The low-energy shift is attributed to the combined effects of an increasing QD size and a decreasing strain inside the QD's with increasing indium concentration in the QW. These two effects will be discussed in detail in the following sections. The trend is seemingly reversed on going from $x=20\%$ to $x=25\%$. As discussed below the partial decomposition of the $\text{In}_x\text{Ga}_{1-x}\text{As}$ layer is most effective for the $x=20\%$ sample, leading to the largest QD's. The reason might be a larger size of the initial InAs islands as suggested by the

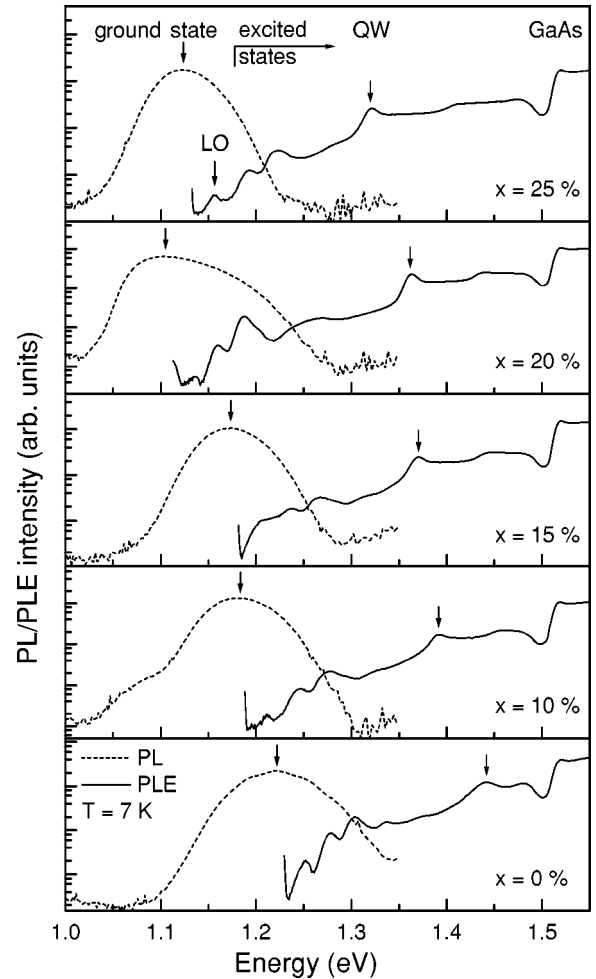


FIG. 2. PL (dashed) and PLE (solid) spectra for InAs QD's overgrown by an $\text{In}_x\text{Ga}_{1-x}\text{As}$ cap layer ($x=0, 10\%, 15\%, 20\%$, and 25%). The PLE spectra were detected at the corresponding PL maxima.

island density, which is $\sim 50\%$ lower than in the other samples. An increased stressor size enhances decomposition.²⁰ Additionally, dislocated clusters appear at the highest indium concentration ($x=25\%$), which are efficient sinks for indium, reducing the average size of the coherent QD's.²⁰

Information on the excited states is obtained from PLE studies. The full lines in Fig. 2 show PLE spectra recorded at the maximum of the corresponding PL peak. The spectra reveal efficient excitation via the QW (marked by arrows), which exhibits with increasing indium content of the $\text{In}_x\text{Ga}_{1-x}\text{As}$ layer a low-energy shift of the same order as that of the QD ground state transition. The energy difference between the QW and the QD ground state is largest for the $x=20\%$ sample supporting an enhanced decomposition of the QW for this sample. The transition energy of the QW can be exploited to estimate the actual indium concentration of the partly decomposed $\text{In}_x\text{Ga}_{1-x}\text{As}$ layer as will be discussed in Sec. IV.

The excitation resonances appearing in an ~ 200 meV energy window above the ground state transition are attributed to the resonant excitation of QD transitions.^{11,12} The

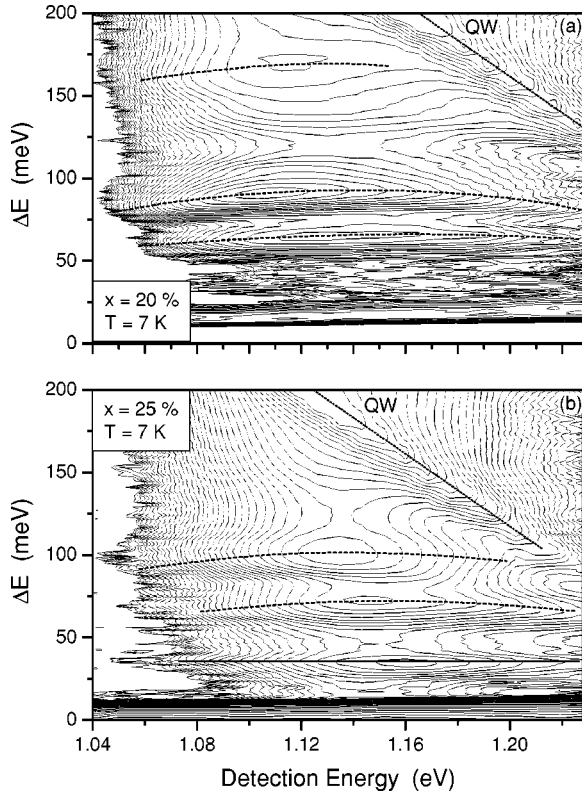


FIG. 3. Contour plots of the logarithmic PL intensity, as a function of the detection and excess excitation energies for the samples with $x=20\%$ (a) and $x=25\%$ (b) indium in the QW.

lowest-energy resonance at ~ 34 meV above the ground state transition is observed for all In(Ga)As QD's and attributed to phonon-assisted absorption.²¹ The energies of the two resonances ~ 70 meV and ~ 100 meV above the ground state transition are close to two and three times the LO-phonon energy. The observation of similar PLE resonances in single-layer InAs/GaAs QD's being independent on the QD size²² has been attributed to multi-LO-phonon resonances, which result from the competition between relaxation and defect-related nonradiative recombination, i.e., the phonon-bottleneck effect. For samples for which such nonradiative recombination is negligible, PLE reveals directly the excited state absorption spectrum and the resonance energies show a quantum-size effect.¹²

Figure 3 shows contour plots of the logarithmic PL intensity for the $x=20\%$ [panel (a)] and $x=25\%$ [panel (b)] samples as a function of the detection energy and the excess excitation energy $\Delta E = E_{\text{excitation}} - E_{\text{detection}}$. Tuning the detection energy across the QD PL peak reveals variations of ~ 6 and ~ 12 meV for the transition energies of the ~ 70 meV and ~ 100 meV resonances, respectively, suggesting recombination-limited dynamics for the investigated samples. Obviously relaxation is sufficiently fast to populate the ground state for all excitation processes in all QD's, i.e., the relaxation yield is close to one and nonradiative recombination is negligible.²³ Thus, the PLE resonances correspond to excited state absorptions of QD's with a given ground state transition energy ($E_{\text{detection}}$), whereby the line-width is a measure of the uniformity of the QD ensemble.

For a given ground state transition energy (i.e., $E_{\text{detection}}$) the combination of size, shape, and composition fluctuations still provides for inhomogeneous broadening of the excited state transitions.²⁴ A comparison of the excited state transition energies in the different samples shows similar quantization despite the pronounced low-energy shift of the ground state transition, supporting a similar lateral confinement, i.e., a similar average QD size. The excited state transition energies in the $x=20\%$ sample are on average ~ 7 meV smaller, indicating a slightly increased average QD size.

Based on the PLE contour plots shown in Fig. 3 two immediate consequences of the lowering of the lateral potential barriers with increasing indium concentration of the QW can be identified. On the one hand, excitation resonances becoming nearly degenerate with the QW show a negative quantum size effect, i.e., the excited state splitting decreases with decreasing QD size. Such an inverse quantum-size effect has recently been observed for higher excited states of larger InAs/GaAs QD's and attributed to the enhanced delocalization of carriers in states nearly degenerate with the two-dimensional WL.¹² The absolute energy of excited state transitions involving such delocalized states is correlated with the QW transition energy and thus depends only little on the QD size, causing a negative quantum-size effect. On the other hand, the low-energy In_xGa_{1-x}As QW limits the number of localized states in the QD's (compare, e.g., Fig. 3). In the $x=25\%$ sample only the components of the $n=1$ excited electron states (at ~ 70 meV and ~ 100 meV) are localized, whereas in the $x=20\%$ sample at least some of the $n=2$ electron states (at ~ 170 meV) are also localized. The enhanced decomposition leads to larger QD's and a higher-energy QW in this sample. The QD's overgrown with an In_xGa_{1-x}As cap layer provide only 6 to 12 bound exciton states, whereas large conventional self-organized InAs QD's might accommodate up to 30 excitons.^{25,26} Furthermore, the low lateral barrier between the QD's is expected to enhance lateral coupling by carrier exchange at elevated temperatures. At the same time, the vertical potential barrier in the growth direction, being crucial for room-temperature luminescence, remains high.

The PL and PLE results support the notion of strain engineering the electronic properties of self-organized InAs QD's by overgrowth with a suitable gallium-rich In_xGa_{1-x}As cap layer. A detailed understanding of the interrelated effects of strain-driven decomposition and strain relaxation is, however, a precondition for the controlled growth of QD structures optimized, e.g., for particular device applications. In the following the experimental results are compared to effective mass calculations for the QW system consisting of the InAs WL and the In_xGa_{1-x}As layer [Fig. 4(a)], and to eight-band $\mathbf{k}\cdot\mathbf{p}$ calculations¹³ for the localized QD states [Fig. 4(b)]. The spatial separation of the QW and QD regions allows us to use independent theoretical models appropriate to the respective lateral extension of the wave function.

IV. DECOMPOSITION OF THE InGaAs LAYER

In the present growth approach, the In_xGa_{1-x}As layer is deposited on an inhomogeneously strained surface whereby

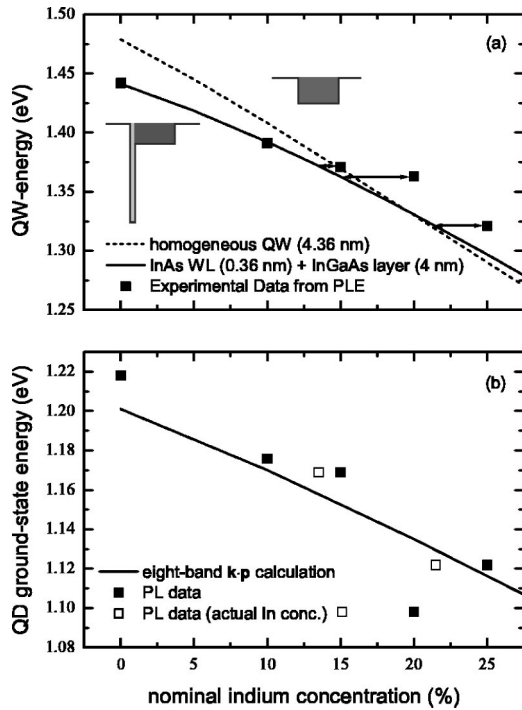


FIG. 4. (a) Experimental (points) and calculated (line) exciton energy of the QW formed by the original wetting layer and the partly decomposed $\text{In}_x\text{Ga}_{1-x}\text{As}$ layer for two structural assumptions: a completely intermixed (dashed line) or a simply sandwiched (full line) structure. The insets depict the two structural assumptions. (b) Symbols represent the experimental ground state transition energies and the line represents the exciton energy calculated in the eight-band $\mathbf{k}\cdot\mathbf{p}$ model assuming a constant QD size.

the predeposited InAs islands act as stressors. Strain-driven surface migration⁸ leads to a preferential incorporation of indium at the already existing InAs islands, increasing the effective size of the QD's.^{15,16} As shown recently, the degree of decomposition depends on the initial island size, the indium concentration, and the growth conditions.²⁰ In the present case of overgrowth with a gallium-rich $\text{In}_x\text{Ga}_{1-x}\text{As}$ cap layer partial decomposition lowers the indium content of the ternary layer. In the ultimate situation of overgrowth with pure InAs the additional InAs aggregates completely at the already existing islands.²⁷

The actual composition of the $\text{In}_x\text{Ga}_{1-x}\text{As}$ layer and therefore the degree of decomposition can be estimated by comparing the ground state transition energy of the QW observed, e.g., in the PLE spectra (Fig. 2), to one-dimensional effective mass model calculations. The dashed and the full lines in Fig. 4(a) represent calculations for the two limiting structural assumptions: The QW formed by the InAs WL and the $\text{In}_x\text{Ga}_{1-x}\text{As}$ layer is assumed to be either completely intermixed or to be simply sandwiched, as indicated schematically by the insets. Note that in the calculations x is the actual indium concentration of the $\text{In}_x\text{Ga}_{1-x}\text{As}$ ternary alloy, which in the case of decomposition will be lower than the nominally deposited one. The thickness of the InAs WL is assumed to be 0.36 nm to match the QW energy in the reference sample ($x=0$). Obviously, both intermixing of the InAs WL with the $\text{In}_x\text{Ga}_{1-x}\text{As}$ layer and decomposition of

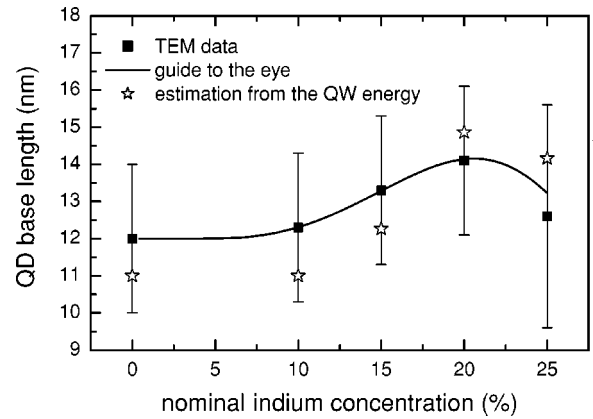


FIG. 5. The QD base lengths estimated from TEM images (Ref. 20) and based on the QW energy as described in the text.

the latter are negligible for $x \leq 10\%$. For indium concentrations above 10% the QW transition is observed at higher energies than predicted for the nominal indium concentration, indicating partial decomposition of the ternary alloy.

Figure 4(a) allows estimation of the actual composition of the grown $\text{In}_x\text{Ga}_{1-x}\text{As}$ layer as indicated by horizontal arrows. Actual indium concentrations of 13.5%, 15.1%, and 21.5% are obtained for the $x=15\%$, $x=20\%$, and $x=25\%$ samples, respectively. The strain-driven decomposition is most efficient in the $x=20\%$ sample. The actual indium concentration provides an estimate for the QD base length based on the lateral QD density and height obtained from TEM images.²⁰ Figure 5 compares the estimated average base length of the QD's to corresponding TEM results, revealing rather good agreement. Obviously, the missing indium is accumulated at the InAs QD's, supporting the concept of strain-driven decomposition due to indium migration to the InAs stressors during the growth of the $\text{In}_x\text{Ga}_{1-x}\text{As}$ cap layer.

For the highest indium concentration ($x=25\%$) the estimated QD base length is larger than the TEM one. A possible explanation is the observed formation of dislocated, partially strain-relaxed clusters,²⁰ which accumulate excessively indium at the expense of the growth of the less favorable coherent islands. With increasing indium concentration of the $\text{In}_x\text{Ga}_{1-x}\text{As}$ layer the increasing strain energy results finally in the formation of dislocations in the 4 nm thick $\text{In}_x\text{Ga}_{1-x}\text{As}$ layer. Additionally, the sensitivity of the decomposition to the initial island size might account at least partly for the increased island size in the $x=20\%$ sample. An $\sim 50\%$ lower island density in this sample suggests that the initial InAs islands were already larger than in the other samples, which favors decomposition. The enhanced decomposition accounts for the lower QD ground state transition energy and the higher-energy QW (Fig. 4). Optimized growth conditions favoring decomposition allow one to access the 1.3 μm spectral region for room-temperature devices.²⁰

V. STRAIN RELAXATION WITHIN THE QUANTUM DOTS

As pointed out above, the electronic structure of the InAs QD's is altered by both the changing effective size of the

InAs QD's (Fig. 5) and the $\text{In}_x\text{Ga}_{1-x}\text{As}$ layer affecting the strain distribution in the final QD structure. For strained Stranski-Krastanow QD's both the chemical potential step at the interfaces and the strain-induced local changes of the band edges are similarly important for the actual confining potential.¹³ The strain distribution, depending on the QD shape and composition, potentially introduces a large variation in the electronic properties of such strained QD's. In particular, the additional $\text{In}_x\text{Ga}_{1-x}\text{As}$ layer introduced in the present growth approach leads to a pronounced modification of the strain distribution and, therewith, of the electronic properties.

To estimate the effects of the altered strain distribution on the electronic properties of the QD's we calculated the strain distribution in the framework of continuum mechanics, using a finite difference method, and the localized QD states, using an eight-band $\mathbf{k}\cdot\mathbf{p}$ model. Exciton formation is treated self-consistently in the Hartree approximation. The fundamentals of the calculations are described in detail for pyramidal InAs/GaAs QD's in Ref. 13 and have recently been demonstrated to successfully explain corresponding experimental results.^{12,21}

For the calculations the QD's were assumed to be truncated InAs pyramids capped by a 4 nm thick $\text{In}_x\text{Ga}_{1-x}\text{As}$ layer of varying composition. The actual indium concentration x in the investigated samples is in general smaller than the nominal one [Fig. 4(a)] as a result of the strain-driven partial decomposition. Note that the decomposition is likely to result in a gradually changing indium profile. However, at the present stage no corresponding structural information is available and thus we consider discrete interfaces between homogeneous materials. Guided by the TEM results, we assumed truncated pyramids with $\{101\}$ -type side facets and a base length (height) of 11.3 nm (2.6 nm), which are located on top of a 0.36 nm thick InAs WL and covered by a 4 nm thick $\text{In}_x\text{Ga}_{1-x}\text{As}$ cap layer of varying composition, as shown schematically in Fig. 1. The decomposition-induced variation of the island size (Fig. 5) is neglected in the calculations to isolate the effects of the strain redistribution.

Figure 6(a) shows the evolution of the hydrostatic strain following a (001) line through the center of the QD in the growth direction (see inset). With increasing indium concentration the hydrostatic strain increases in the QW but decreases in the QD's and in the GaAs barrier. The $\text{In}_x\text{Ga}_{1-x}\text{As}$ layer reduces the strain within the QD's and at the surface of the cap layer, allowing the growth of multiple layers of uncoupled QD's.²⁰ The decreasing hydrostatic strain within the QD's leads to a lowering of the confining potential, as shown in Fig. 6(b) for the conduction band. The potential becomes deeper with increasing indium concentration following the strain dependence of the InAs band gap. The average conduction (valence) band potential in the QD decreases (increases) by ~ 63 meV (~ 44 meV) on increasing x to 30%, which transfers directly into a corresponding decrease (increase) of the electron (hole) ground state energy. In the $\text{In}_x\text{Ga}_{1-x}\text{As}$ layer the increasing indium content leads to a lowering of the band gap, which is only partly compensated by the increasing hydrostatic strain. The $\text{In}_x\text{Ga}_{1-x}\text{As}$ layer

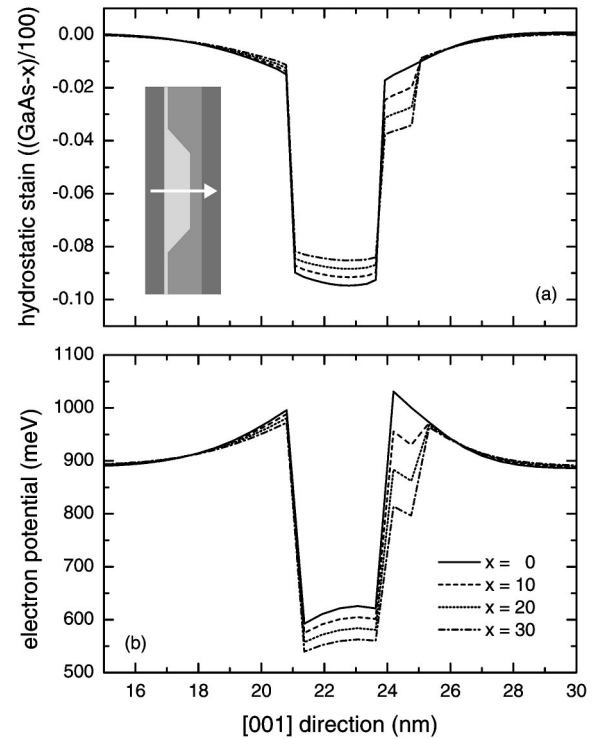


FIG. 6. Profile of the hydrostatic strain (a) and the electron potential (b) along a line through the center of the dot in the growth direction for different indium concentrations.

lowers the lateral barrier between QD's, maintaining the high barrier in the growth direction. However, the reduced lateral barrier has only negligible direct effect on the strongly localized electron and hole states.

The wave functions of the four lowest electron and hole states are shown in Fig. 7 for $x=0$, being representative for

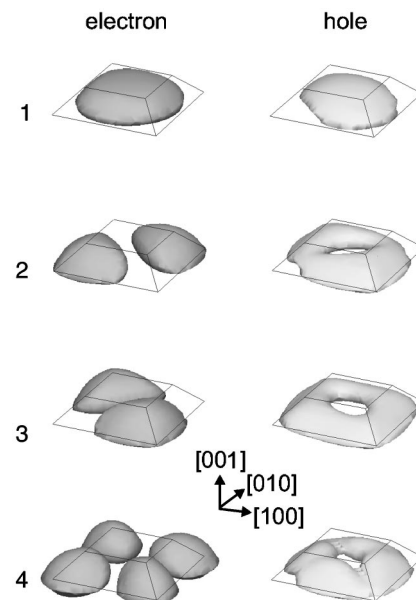


FIG. 7. Electron and hole wave functions predicted by eight-band $\mathbf{k}\cdot\mathbf{p}$ calculations for a truncated InAs pyramid ($x=0$).

the studied composition range of the $\text{In}_x\text{Ga}_{1-x}\text{As}$ layer. The wave functions for the truncated pyramidal InAs QD are similar to those of a pyramidal one.¹³ However, the smaller side facets and shorter edges provide for a weaker piezoelectric potential. In consequence, the p -type contribution to the hole ground state is less pronounced and the splitting of the first two excited electron states is negligible (<3 meV). The truncated shape enhances the oscillator strength of the ground state transition in good agreement with recent experimental results.²⁸

The line in Fig. 4(b) represents the predicted evolution of the exciton ground state transition energy as a function of the indium concentration. The redistribution of the strain causes a low-energy shift of the ground state transition energy by ~ 65 meV on increasing x to 20%, which is in qualitative agreement with the experimental results (solid squares). However, taking into account the actual indium concentration (open squares) it is obvious that, in particular for the $x=20\%$ sample, the increased island size also contributes to the redshift. Nevertheless, for the investigated samples the strain redistribution provides the major contribution to the observed redshift. The partial decomposition of the $\text{In}_x\text{Ga}_{1-x}\text{As}$ layer reduces the strain relaxation in the QD's whereas the simultaneously increasing QD size decreases the quantum confinement. The two effects are counteracting and partly compensate each other with respect to the ground state transition energy. Only in the case of pronounced decomposition as for the $x=20\%$ sample will the lowering of the quantization dominate and enhance the redshift. Optimized growth conditions, enhancing decomposition, allow the achievement of low-energy shifts of up to 200 meV of the QD ground state transition,²⁰ providing access to the 1.3 μm spectral region.

The size, i.e., the base length, of the QD's is inversely related to the excited state splitting via the quantum size effect.^{12,13} However, the excited state splitting as observed in PLE experiments (Fig. 2 and Fig. 3) remains almost unchanged on increasing the indium concentration despite the large low-energy shift of the ground state transition energy, supporting a similar average QD size in the different samples (compare Fig. 5). Figures 8(a) and 8(c) show the predicted absorption spectra for $x=0$ and $x=30\%$. The exciton transitions are represented by bars whose length corresponds to the oscillator strength. Additionally, absorption spectra predicted for 10 meV inhomogeneous broadening are shown for a better comparison with the PLE experiments.

In addition to the ground state ($e1-h1$) transition the eight-band $\mathbf{k}\cdot\mathbf{p}$ calculations predict three major transition groups, which could not be resolved in the PLE experiments. The first one ~ 70 meV above the ground state transition is composed of the dominant $e2-h2$ and the $e3-h2$ transitions. The second one at ~ 85 meV consists of the four possible transitions between $e2$, $e3$, $h3$, and $h4$. Finally, the one at ~ 135 meV consists of the $e4-h4$ and the dominant $e3-h4$ transition. The first and the second line groups are close to the observed excited state transitions at ~ 60 and ~ 85 meV. The discrepancy in the absorption strength (compare Fig. 2) is attributed to the idealized QD shape assumed in the calcu-

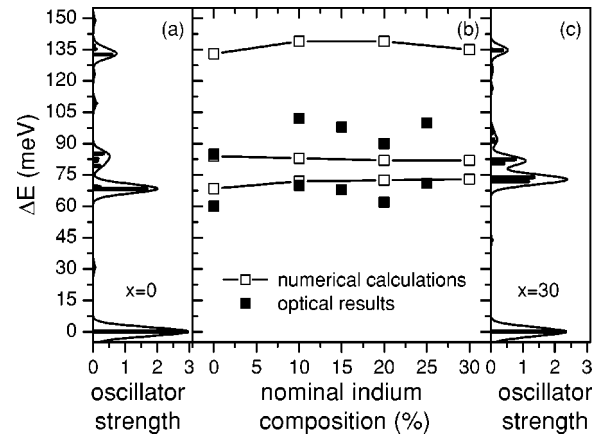


FIG. 8. Oscillator strengths (bars) and absorption spectra artificially broadened by 10 meV (solid line) predicted by eight-band $\mathbf{k}\cdot\mathbf{p}$ calculations for $x=0$ (a) and $x=30\%$ (c). (b) Excited state energies from the eight-band $\mathbf{k}\cdot\mathbf{p}$ calculation (lines with open symbols) and PLE spectra (solid symbols).

lations. Figure 8(b) compares the predicted and observed excited state transition energies as a function of the indium concentration. The predicted energies change smoothly by a few meV mainly due to the altered strain distribution, which lowers the effect of the piezoelectric potential on the hole states. The experimentally observed energies depend as well only weakly on the indium concentration, showing no systematic trend. The slightly smaller energies in the $x=20\%$ sample are consistent with the increased average QD size and demonstrate the sensitivity of the quantization to the lateral confinement, i.e., the size of the QD's.

VI. CONCLUSION

In conclusion, we have investigated the optical properties and analyzed the electronic properties of InAs QD's overgrown by an $\text{In}_x\text{Ga}_{1-x}\text{As}$ layer. The properties are strongly influenced by the strain-driven partial decomposition of the $\text{In}_x\text{Ga}_{1-x}\text{As}$ layer, which increases the effective QD size, and by the altered strain distribution in the final structure. Both effects contribute to the observed low-energy shift of the QD ground state transition and can be controlled via the growth-condition-dependent decomposition. For the assumed QD size and shape, the lowering of the potential within the QD's due to the strain redistribution contributes ~ 65 meV to the observed low-energy shift of the ground state transition for $x=20\%$.

The overgrowth of InAs QD's with a gallium-rich $\text{In}_x\text{Ga}_{1-x}\text{As}$ cap layer is a potentially advantageous means to use strain to engineer the electronic properties of self-organized InAs/GaAs QD's. The ground state transition energy can be decreased maintaining a large substrate splitting, and, additionally, the low-energy QW limits the number of localized states and enhances the lateral coupling of QD's by thermal emission and recapture. All three effects are beneficial for laser devices and might contribute to the success of corresponding device structures.¹⁵

ACKNOWLEDGMENTS

Parts of this work were supported by Deutsche Forschungsgemeinschaft in the framework of SFB 296, NanOp

Competence Center, and INTAS. Parts of the electronic structure calculations were performed on the Cray T3E computer of the Konrad-Zuse-Zentrum für Informationstechnik Berlin within Project No. Bvpt13.

- *On leave from A. F. Ioffe Physicotechnical Institute, St. Petersburg, Russia.
- ¹D. Bimberg, M. Grundmann, and N. N. Ledentsov, *Quantum Dot Heterostructures* (J. Wiley & Sons, Chichester, 1999).
- ²M. Grundmann, *Physica E* (Amsterdam) **5**, 167 (2000).
- ³D. Bimberg, N. Kirstaedter, N.N. Ledentsov, Z.I. Alferov, P.S. Kop'ev, and V.M. Ustinov, *IEEE J. Sel. Top. Quantum Electron.* **3**, 197 (1997).
- ⁴J.J. Finley, M. Skalitz, M. Arzberger, A. Zrenner, G. Böhm, and G. Abstreiter, *Appl. Phys. Lett.* **73**, 2618 (1998).
- ⁵J.C. Campbell, D.L. Huffaker, H. Deng, and D.G. Deppe, *Electron. Lett.* **33**, 1337 (1997).
- ⁶F. Heinrichsdorff, M. Grundmann, O. Stier, A. Krost, and D. Bimberg, *J. Cryst. Growth* **195**, 540 (1998).
- ⁷S. Fafard and C.N. Allen, *Appl. Phys. Lett.* **75**, 2374 (1999).
- ⁸Q. Xie, A. Madhukar, P. Chen, and N.P. Kobayashi, *Phys. Rev. Lett.* **75**, 2542 (1995).
- ⁹N.N. Ledentsov, V.A. Shchukin, M. Grundmann, N. Kirstaedter, J. Böhrer, O. Schmidt, D. Bimberg, V.M. Ustinov, A.Y. Egorov, A.E. Zhukov, P.S. Kop'ev, S.V. Zaitsev, N.Y. Gordeev, Z.I. Alferov, A.I. Borovkov, A.O. Kosogov, S.S. Ruvimov, P. Werner, U. Gösele, and J. Heydenreich, *Phys. Rev. B* **54**, 8743 (1996).
- ¹⁰I. Mukhametzhanov, R. Heitz, J. Zeng, P. Chen, and A. Madhukar, *Appl. Phys. Lett.* **73**, 1841 (1998).
- ¹¹R. Heitz, I. Mukhametzhanov, A. Madhukar, A. Hoffmann, and D. Bimberg, *J. Electron. Mater.* **28**, 520 (1999).
- ¹²R. Heitz, O. Stier, I. Mukhametzhanov, A. Madhukar, and D. Bimberg, *Phys. Rev. B* **62**, 11 017 (2000).
- ¹³O. Stier, M. Grundmann, and D. Bimberg, *Phys. Rev. B* **59**, 5688 (1999).
- ¹⁴H. Fu, L.-W. Wang, and A. Zunger, *Phys. Rev. B* **59**, 5568 (1999).
- ¹⁵A.E. Zhukov, A.R. Kovsh, N.A. Maleev, S.S. Mikhrin, V.M. Ustinov, A.F. Tsatsul'nikov, M.V. Maximov, B.V. Volovik, D.A. Bedarev, Y.M. Shernyakov, P.S. Kop'ev, Z.I. Alferov, N.N. Ledentsov, and D. Bimberg, *Appl. Phys. Lett.* **75**, 1926 (1999).
- ¹⁶M.V. Maximov, A.F. Tsatsul'nikov, B.V. Volovik, D.A. Bedarev, A.E. Zhukov, A.R. Kovsh, N.A. Maleev, V.M. Ustinov, P.S. Kop'ev, Z.I. Alferov, R. Heitz, N.N. Ledentsov, and D. Bimberg, *Physica E* (Amsterdam) **7**, 326 (2000).
- ¹⁷K. Nishi, H. Saito, S. Sugou, and J.-S. Lee, *Appl. Phys. Lett.* **74**, 1111 (1999).
- ¹⁸H.Y. Liu, X.D. Wang, B. Xu, D. Ding, W.H. Jiang, J. Wu, and Z.G. Wang, *J. Cryst. Growth* **213**, 193 (2000).
- ¹⁹N.-T. Yeh, T.-E. Nee, J.-I. Chyi, T.M. Hsu, and C.C. Huang, *Appl. Phys. Lett.* **76**, 1567 (2000).
- ²⁰M.V. Maximov, A.F. Tsatsul'nikov, B.V. Volovik, D.S. Sizov, Y.M. Shernyakov, I.N. Kaiander, A.E. Zhukov, A.R. Kovsh, S.S. Mikhrin, V.M. Ustinov, Z.I. Alferov, R. Heitz, V.A. Shchukin, N.N. Ledentsov, D. Bimberg, Y.G. Musikhin, and W. Neumann, *Phys. Rev. B* **62**, 16 671 (2000).
- ²¹R. Heitz, I. Mukhametzhanov, O. Stier, A. Madhukar, and D. Bimberg, *Phys. Rev. Lett.* **83**, 4654 (1999).
- ²²R. Heitz, M. Veit, N.N. Ledentsov, A. Hoffmann, D. Bimberg, V.M. Ustinov, P.S. Kop'ev, and Z.I. Alferov, *Phys. Rev. B* **56**, 10 435 (1997).
- ²³Nonradiative recombination channels can be introduced artificially by adding aluminum to the $\text{In}_x\text{Ga}_{1-x}\text{As}$ cap layer. For such samples the intensity of the near-resonant PLE resonances observed at low excitation density decreases by more than one order of magnitude and the resonances become narrower as a result of the competition between relaxation and nonradiative recombination (Ref. 20).
- ²⁴R. Heitz, A. Kalburge, Q. Xie, M. Grundmann, P. Chen, A. Hoffmann, A. Madhukar, and D. Bimberg, *Phys. Rev. B* **57**, 9050 (1998).
- ²⁵S. Raymond, X. Guo, J.L. Merz, and S. Fafard, *Phys. Rev. B* **59**, 7624 (1999).
- ²⁶R. Heitz, F. Guffarth, I. Mukhametzhanov, M. Grundmann, A. Madhukar, and D. Bimberg, *Phys. Rev. B* **62**, 16 881 (2000).
- ²⁷I. Mukhametzhanov, Z. Wei, R. Heitz, and A. Madhukar, *Appl. Phys. Lett.* **75**, 85 (1999).
- ²⁸R. Heitz, H. Born, T. Lüttgert, A. Hoffmann, and D. Bimberg, *Phys. Status Solidi B* **221**, 65 (2000).